HHS Public Access

Author manuscript

J Cell Physiol. Author manuscript; available in PMC 2017 March 01.

Published in final edited form as:

J Cell Physiol. 2016 March ; 231(3): 568–575. doi:10.1002/jcp.25100.

RhoA-Mediated Functions in C3H10T1/2 Osteoprogenitors Are Substrate Topography Dependent

Yoichiro Ogino[1,2], **Ruiwei Liang**[1], **Daniela B. S. Mendonça**[3], **Gustavo Mendonça**[3], **Masako Nagasawa**[1,4], **Kiyoshi Koyano**[2], and **Lyndon F. Cooper**[1]

[1]Department of Prosthodontics, School of Dentistry, University of North Carolina at Chapel Hill, Chapel Hill, North Carolina

[2]Division of Oral Rehabilitation, Faculty of Dental Science, Kyushu University, Fukuoka, Japan

[3]Division of Prosthodontics, School of Dentistry, University of Michigan, Ann Arbor, Michigan

[4]Division of Bio-Prosthodontics, Niigata University Graduate School of Medical and Dental Sciences, Niigata, Japan

Abstract

Surface topography broadly influences cellular responses. Adherent cell activities are regulated, in part, by RhoA, a member of the Rho-family of GTPases. In this study, we evaluated the influence of surface topography on RhoA activity and associated cellular functions. The murine mesenchymal stem cell line C3H10T1/2 cells (osteoprogenitor cells) were cultured on titanium substrates with smooth topography (S), microtopography (M), and nanotopography (N) to evaluate the effect of surface topography on RhoA-mediated functions (cell spreading, adhesion, migration, and osteogenic differentiation). The influence of RhoA activity in the context of surface topography was also elucidated using RhoA pharmacologic inhibitor. Following adhesion, M and N adherent cells developed multiple projections, while S adherent cells had flattened and widespread morphology. RhoA inhibitor induced remarkable longer and thinner cytoplasmic projections on all surfaces. Cell adhesion and osteogenic differentiation was topography dependent with S < M and N surfaces. RhoA inhibition increased adhesion on S and M surfaces, but not N surfaces. Cell migration in a wound healing assay was greater on S versus M versus N surfaces and RhoA inhibitor increased S adherent cell migration, but not N adherent cell migration. RhoA inhibitor enhanced osteogenic differentiation in S adherent cells, but not M or N adherent cells. RhoA activity was surface topography roughness dependent (S < M, N). RhoA activity and -mediated functions are influenced by surface topography. Smooth surface adherent cells appear highly sensitive to RhoA function, while nano-scale topography adherent cell may utilize alternative cellular signaling pathway(s) to influence adherent cellular functions regardless of RhoA activity.

Corresponding Authors: Yoichiro Ogino, Division of Oral Rehabilitation, Faculty of Dental Science, Kyushu University, 3-1-1 Maidashi, Higashi-ku, Fukuoka, Japan, ogino@dent.kyushu-u.ac.jp. Lyndon F. Cooper, Department of Prosthodontics, School of Dentistry, University of North Carolina at Chapel Hill, 4610 Koury Oral Health Sciences Building, CB# 7450, Chapel Hill, CB #7450, Chapel Hill, NC 27599-7450, Lyndon_Cooper@unc.edu.

Dental implant surface topography modulates osteoblast function and influences interfacial bone formation supporting osseointegration (Cooper *et al.*, 1999; Mendonça *et al.*, 2008). Micron scale topographic surface modification increases cell adhesion, proliferation, and differentiation and has been widely adopted for clinical use (Nanci *et al.*, 1998; Cooper *et al.*, 2006). Recent studies indicated that nanoscale modification further influences cellular differentiation and improve the osseointegration process (Mendonça *et al.*, 2009, 2010; Khatiwala *et al.*, 2009; Kulangara *et al.*, 2012; Salou *et al.*, 2015). The mechanisms responsible for topography-mediated cell responses, especially involving the nano-structured surface, are not fully elucidated.

Cell adhesion influences subsequent cellular functions. The roles of the extracellular matrix, cytoskeleton and membrane receptors are well characterized (Huveneers and Danen, 2009). Cell attachment involves integrin receptor engagement of adsorbed extracellular matrix components. In a cell-type and substrate-specific manner, integrin heterodimers activate downstream signaling pathways including the Rho-family of GTPases (McBeath *et al.*, 2004). RhoA modulates cell adhesion, motility, and morphology (de Curtis and Meldolesi, 2012; Lessey *et al.*, 2012, Hamamura *et al.*, 2012). RhoA can be activated in response to mechanical force (Etienne-Manneville and Hall, 2002) and this process has been implicated in the control of osteoblast (Galli *et al.*, 2012) and mesenchymal cell fate (Passeri *et al.*, 2010). Surface topography also influences cell morphology via cytoskeleton remodeling and maintenance of topography-specific adhesion (Seo *et al.*, 2011, 2014; Prowse *et al.*, 2013). The present study tests our hypothesis that RhoA activity may be differentially influenced by micron and nanoscale topography during cell adhesion and spreading and this further influences adherent cellular functions on the modeled implant surface.

Materials and Methods

Disk surface preparation

Commercially pure grade IV titanium disks were prepared as previously described (Mendonça *et al.*, 2009, 2010). Briefly, smooth (S) surfaces were polished to 600 grit. Micron (M) surfaces were prepared by a second step of 100-μm aluminum oxide (Al2O3) particle blasting and 5N HCl treatment. Nano (N) surfaces further treated 50/50 v/v % solution of 30% H2O2 and 2N H2SO4 for 2 h (Mendonça *et al.*, 2010).

Surface analysis

Prepared disks were examined by high-resolution scanning electron microscopy (Field Emission Scanning Electron Microscope [FEG-SEM; SEM, Hitachi S-4700, Tokyo, Japan]). For measuring roughness, a laser scanning microscope (VK-9710, Keyence, Osaka, Japan) was used. Measurements were made at five different points on the disk surfaces and average values were calculated.

Cell culture

C3H10T1/2, murine mesenchymal stem cells, were grown in Dulbecco's Modified Eagle's Medium (DMEM; Lonza, Walkersville, MD) with 10% fetal bovine serum (FBS) and 1% antibiotics and antimycotic solution (Sigma, St. Loius, MO) in a 5%CO2 incubator at 37°C.

Where indicated, the RhoA inhibitor, cell-permeable C3 transferase (C3; Cytoskeleton, Denver, CO) was added during culture.

Assessment of cell morphology by immunofluorescent staining

Cells were seeded onto S, M, and N disks in 12-well culture plates with or without 500 ng/ml C3 (cell density: 1 × 105 cells/well). At 2 and 6 h post-seeding, the cells were washed twice with PBS and fixed for 10 min with 4% paraformaldehyde followed by incubation with PBS containing with 1% bovine serum albumin to reduce nonspecific background staining. The cells were incubated with monoclonal anti-vinculin FITC (Sigma) followed by phalloidin (Texas Red®-X phalloidin, Invitrogen, Grand Island, NY) to detect the actin cytoskeleton. The nuclei were stained with ProLong® Gold antifade reagent with DAPI (Invitrogen, Grand Island, NY). Images were acquired with Olympus IX51 (Olympus, Tokyo, Japan).

Cell adhesion assay

Cells were passaged and seeded onto S, M, or N disks (in 96-well culture plates) at a density of 1 × 104 cells/well in DMEM with 3% FBS (control) or with C3 added at a final concentration of 50 or 500 ng/ml. After 2 and 6 h of incubation, disks were washed twice with PBS to remove non-adherent cells. The number of attached cells was determined using CellTiter 96® AQueous One Solution Reagent (MTS; Promega, Madison, WI).

Cell migration assay (scratch assay)

Cells were seeded onto disks in 12-well culture plates at a density of 1 × 105 cells/well and cultured with DMEM containing 10% FBS. After 24 h, the culture media was changed to DMEM containing 3% FBS (control) and DMEM with 3% FBS and 500 ng/ml C3. Twelve hours later, cell layers were scratched with a pipette tip. After 4, 8, 12, and 16 h, the cell layers were photographed after immunofluorescent staining with fluorescent phallotoxins (described above). The area of cell migration and rate of closure (wound healing rate) was calculated with Image J (n = 6 fields; National Institutes of Health, Bethesda, MD).

Osteogenic differentiation assay in the presence or absence of RhoA inhibitor

Cells were seeded onto S, M, or N disks into 12-well culture plates (cell density: 1 × 105 cells/well) and 24 h later, media was changed to osteogenic media (OST media, 10 mM glycerophosphate, 0.2 mM ascorbic acid and 10 nM dexamethasone) with or without C3 (500 ng/ml) and replaced every 3 days. Adherent cells total RNA was prepared (Trizol®, Invitrogen) and osteogenesis-related mRNA (alkaline phosphatase [ALP], Osterix [OSX], Collagen I [Col I], and Runx2) expression was measured by quantative real-time reverse transcriptional polymerase chain reaction (RT-PCR, Taqman® Universal PCR master Mix, Applied Biosystems, Branchburg, NJ). Using primers for ALP (Mm00475831), Col I (Mm00801666), OSX (Mm00504574) and Runx2 (Mm00501578) and GAPDH (Cat.#4308313, Applied Biosystems, Foster City, CA). RT-PCR was performed in triplicate using ABI 7200 real-time thermocycler (Applied Biosystems).

RhoA activity assays

RhoA activation was measured in cells seeded onto S, M, and N disks in 12-well culture plates (cell density: 1 × 105 cells/well) with or without 500 ng/ml C3. At 1, 2, 6, and 24 h post-seeding, RhoA activity was measured as GTP-bound RhoA (G-LISA RhoA activation assay kit, Cytoskeleton). Cells were cultured for 12 h after the change of medium containing 3% FBS with or without C3 (500 ng/ml) and 9 scratches/disk were made to stimulate cell motility. After 10 and 30 min, and 1, 2, 4, 8, 12, and 16 h of culture, the level of GTP-loaded RhoA was measured. The experiments were repeated in cells cultured in OST media after 3 and 7 days of culture.

Statistical analysis

All data are presented as the mean ± standard deviation. The statistical analyses for comparing the difference between every surface without C3 treatment were performed with one way ANOVA followed by Scheffe post-test and differences were considered significant at $P < 0.05$. To analyze the effect of RhoA inhibitor on cellular responses statistically, t test was used to compare between non-treated and C3-treated cells on each surface and differences were also considered significant at $P < 0.05$.

Results

Surface analysis

SEM images revealed distinct topographies for the S, M, and N disks. S surfaces showed a linear roughness pattern related to the polishing process (Fig. 1A). M surfaces displayed anisotropic pit-like roughness of micron scale (Fig. 1B). N surfaces revealed sharper ridges and superimposed densely arrayed, nanofeatures (<100 nm) not observed on S and M surfaces (Fig. 1C). The measurement of roughness parameters Ra (arithmetic roughness, Fig. 1D) demonstrated that the highest roughness values were observed with M surfaces, followed by N and S surfaces. Significant differences were detected between each surface.

Cell morphology and RhoA activity during spreading

Cell morphology was influenced by topography and RhoA inhibition. S adherent cells were round, with peripheral vinculin staining at 2 h (Fig. 2A). At 6 h, well-spread cells exhibited stress fibers and vinculin positive focal contacts prominently at the cell periphery (Fig. 2B). C3-treated S adherent cells demonstrated long and thin protrusions with vinculin localized to the extensions (Fig. 2C and D). On M and N surfaces, polygonal cells were observed at 2 h. Cells formed cytoplasmic projections at 2 h (Fig. 2E and I). Vinculin labeling was found at the periphery of the cell and around nuclei. At 6 h, more cellular extensions were observed on both surfaces (Fig. 2F and J). Although RhoA inhibitor treated -M and -N adherent cells did not show remarkable changes in their morphology at 2 h (Fig. 2G and K), they displayed multiple longer and thinner projections at 6 h (Fig. 2H and L). RhoA activities during adhesion were surface roughness dependent. The highest activity was observed in M adherent cells at 1 h and was sensitive to C3 treatment (Fig. 2M). S adherent cells demonstrated increased RhoA activity over 24 h that was C3 inhibited. RhoA activity in N adherent cells increased at 2 and 6 h but showed little sensitivity to C3 treatment until 24 h

(P < 0.01; Fig. 2M). RhoA activity at 24 h was statistically different between non-treated and C3-treated cells for all surfaces (P < 0.01; Fig. 2M).

Cell adhesion assay

After 2 h, the number of cells seeded on M surfaces was significantly increased compared to S surfaces (P < 0.05; Fig. 3A). At 6 h, higher numbers of attached cells were similarly observed on all surfaces. Six hour C3 treatment increased adhesion for S (P < 0.01) and M (P < 0.01) surface adherent cells compared to non-treated cells, whereas increased adhesion was not detected in N adherent cells treated with C3 (Fig. 3B), although C3 treatment did not influence cell adhesion at 2 h (not shown).

Cell migration assay (scratch assay) and RhoA activity during migration

Figure 4A showed the location of cells immediately following wounding (0 h) on S, M, and N surfaces. Topography-specific migration was observed with S > M > N (Fig. 4B and D). RhoA inhibition increased migration of S adherent cells at 8, 12, and 16 h. On M surfaces, C3 treatment significantly increased cell migration only after 16 h. N adherent cell migration was not influenced by C3 treatment. (Fig. 4C and E) The measurement of migration-related activation of RhoA in wounded cell layers demonstrated temporal changes at 4 h for all surfaces. Modest topography-specific differences were measured only at 10 min and 4 h following wounding (Fig. 4F). Treatment with C3 resulted in significant reductions of similar magnitude for RhoA activity following wounding for all groups (Fig. 4G). Reductions were immediate for S adherent cells (P < 0.01), while reductions were not observed until 30 min after wounding for M and N adherent cells (P < 001).

Effect of RhoA inhibitor on osteogenic gene expression and RhoA activation during osteogenic differentiation

The differentiation assay at the level of APL, Col I Osx, and RunX2 revealed a topography dependent differentiation with ALP, OSX, and RUNX2 expressions elevated on M and N surfaces (Fig. 5A). RhoA inhibition significantly enhanced ALP and OSX expression in S adherent cells (Fig. 5B). RhoA inhibition significantly down-regulated Runx2 expression on N surfaces. The measurement of RhoA activity in C3-treated cells under the influence of osteogenic differentiation revealed significant reduction on all surfaces after 3 and 7 days of culture (Fig. 5C and D).

Discussion

Cell morphology and cytoskeletal integrity influence both cell fate and functions (McBeath *et al.*, 2004). Surface topography is one determinant of cell morphology and influences morphology-dependent cellular functions including differentiation (Passeri *et al.*, 2010; Seo *et al.*, 2011, 2014; Galli *et al.*, 2012; Prowse *et al.*, 2013). Recent surface topography developments of endosseous dental implants include both micron-scale and nanometer-scale topographic embellishments that result in increased adherent osteoprogenitor cell differentiation and increased interfacial bone formation (Nanci *et al.*, 1998; Cooper *et al.*, 2006; Mendonça *et al.*, 2009, 2010; Khatiwala *et al.*, 2009; Kulangara *et al.*, 2012; Salou *et al.*, 2015). In cell biology, it is well known that cell morphology and the cytoskeleton

organization are regulated by the Rho-family of GTPases (McBeath *et al.*, 2004; Huveneers and Danen, 2009; Khatiwala *et al.*, 2009; Lessey *et al.*, 2012). Given the emergent role of RhoA GTPase in the determination of cell functions, the present study was designed to explore possible correlations between surface topography, RhoA activity and their effects on cellular functions. Here, different substrate specific adhesion and cell morphology were associated with different levels of RhoA activity. On S surfaces, adherent cells appear highly sensitive to RhoA function for spreading, motility and differentiation. C3H10T1/2 RhoA activity and -mediated functions were substrate specific such that M and N adherent cells were less sensitive to C3 inhibition of RhoA.

Other investigations have explored osteoblast/osteoprogenitor cell interactions on the substrates of different topography with respect to RhoA activity. Both ROCK (a well-known effector of RhoA) inhibition of Wnt/β-catenin signaling and the expression of osteogenic markers are modulated by surface topography (Galli *et al.*, 2012). Seo *et al.* (2011) examined cell adhesion on lattice like micropatterned substrates and demonstrated that the RhoA pathway is critical in topography-induced focal adhesion (FA) formation, actin organization and FA kinase (FAK) phosphorylation. Further, they also demonstrated that the enhancement of FA by a tailor-made micropit surface could upregulate osteogenic differentiation (Seo *et al.*, 2014). In an investigation of osteoblast adhesion on pre-treated and grit blasted/acid etched titanium substrates (SLA), inhibition of ROCK also reduced FA formation and altered downstream signaling resulting in increased Runx-2 activity and osteoblast differentiation (Prowse *et al.*, 2013). The topography dependent reduction of RhoA activity and its influence on adherent cell osteoblastic differentiation was suggested to be a result of changes in the cytoskeleton. They suggest a complex regulatory scenario exists that involves GTPase and ROCK signaling for MSC commitment and differentiation to osteoblasts, but its suppression for the terminal differentiation of osteoblasts (Prowse *et al.*, 2013). The present results suggest that surface topography may modulate RhoA activity directly to influence events beyond adhesion and motility that include differentiation.

The present demonstration that RhoA inhibition altered spreading on S and M surfaces affirms previous findings that cell spreading and morphology are surface topography dependent (Passeri *et al.*, 2010; Galli *et al.*, 2012; Prowse *et al.*, 2013). The greater initial spreading of S adherent cells versus M and N adherent cells was associated with relatively low RhoA activity in S adherent cells compared with M and N adherent cells. Further, the pharmacological inhibiton of RhoA increased the cell adhesion to S and M surfaces, but not N surfaces. This was accompanied by a relative insensitivity of N adherent cells' RhoA activity to C3 treatment (Fig. 2M) at early time points.

A functional consequence of this different signaling pathway may be expressed in cell migration observed in the in vitro wounding assays. That the migration rates were greatest for S adherent cells and increased statistically when S adherent cells were treated with C3 (Fig. 4E) suggests that RhoA function may be central to the motility in S and M adherent cells, but not N adherent cells.

It is widely recognized that cell adhesion influence stem cell fate through changes in cell shape and RhoA activity (McBeath *et al.*, 2004). These experiments confirmed that

osteoprogenitor cell differentiation was increased in cells adherent to M and N surfaces when compared to S adherent cells. C3 treatment (RhoA inhibition) increased differentiation only in S adherent cells. Previous studies using knockdown of RhoA gene and ARHGEF3 (the Rho guanine nucleotide exchange factor activating RhoGTPase) in Saos-2 osteoblast-like cells demonstrated the upregulation of osterix and alkaline phosphatase suggesting upregulation of osteogenesis (Mullin *et al.*, 2014). N surface adherent cell responses (including increased differentiation) differ in the responses mediated by RhoA and its inhibition by C3. This is suggested by the differential responses observed in adhesion and migration in cells adherent to different topography.

These experiments demonstrated topography-specific modulation of RhoA activity and related function. While RhoA appears to be involved in cuing of substrate signals that are known to affect osteogenic differentiation through the cytoskeleton, additional topography-related changes in cytoskeletal organization may influence subsequent signaling pathways utilized in control of cell physiology. Further investigations are needed to elucidate the discrete selection of signaling pathways active in micro- versus nano-scale adherent cells that promote osteoblastic differentiation.

Acknowledgments

This work was supported by the NIH grant (NIH/NIDCR R90DE022527). The authors declare no potential conflicts of interest with respect to the authorship and/or publication of this article. We are grateful to Dr. Amar Shankar Kumar for SEM analysis and Dr. Mami Miyazaki for surface roughness measurement. We also thank Ms. Katherine Avanesyan for preparing disks for this experiment.

References

Cooper LF, Masuda T, Whitson SW, Yliheikkila P, Felton DA. Formation of mineralizing osteoblast cultures on machined, titanium oxide grit-blasted, and plasma-sprayed titanium surfaces. Int J Oral Maxillofac Implants. 1999; 14:37–47. [PubMed: 10074750]

Cooper LF, Zhou Y, Takebe J, Guo J, Abron A, Holmen A, Ellingsen JE. Fluoride modification effects on osteoblast behavior and bone formation at TiO2 grit-blasted c.p. titanium endosseous implants. Biomaterials. 2006; 27:926–936. [PubMed: 16112191]

de Curtis I, Meldolesi J. Cell surface dynamics—How Rho GTPases orchestrate the interplay between the plasma membrane and the cortical cytoskeleton. J Cell Sci. 2012; 125:4435–4444. [PubMed: 23093576]

Etienne-Manneville S, Hall A. Rho GTPases in cell biology. Nature. 2002; 420:629–635. [PubMed: 12478284]

Galli C, Piemontese M, Lumetti S, Ravanetti F, Macaluso GM, Passeri G. Actin cytoskeleton controls activation of Wnt/β-catenin signaling in mesenchymal cells on implant surfaces with different topographies. Acta Biomater. 2012; 8:2963–2968. [PubMed: 22564787]

Hamamura K, Swarnkar G, Tanjung N, Cho E, Li J, Na S, Yokota H. RhoA-mediated signaling in mechanotransduction of osteoblasts. Connect Tissue Res. 2012; 53:398–406. [PubMed: 22420753]

Huveneers S, Danen EH. Adhesion signaling—Crosstalk between integrins, Src and Rho. J Cell Sci. 2009; 122:1059–1069. [PubMed: 19339545]

Khatiwala CB, Kim PD, Peyton SR, Putnam AJ. ECM compliance regulates osteogenesis by influencing MAPK signaling downstream of RhoA and ROCK. J Bone Miner Res. 2009; 24:886–898. [PubMed: 19113908]

Kulangara K, Yang Y, Yang J, Leong KW. Nanotopography as modulator of human mesenchymal stem cell function. Biomaterials. 2012; 33:4998–5003. [PubMed: 22516607]

Lessey EC, Guilluy C, Burridge K. From mechanical force to RhoA activation. Biochemistry. 2012; 51:7420–7432. [PubMed: 22931484]

McBeath R, Pirone DM, Nelson CM, Bhadriraju K, Chen CS. Cell shape, cytoskeletal tension, and RhoA regulate stem cell lineage commitment. Dev Cell. 2004; 6:483–495. [PubMed: 15068789]

Mendonça G, Mendonça DB, Aragão FJ, Cooper LF. Advancing dental implant surface technology—from micron- to nanotopography. Biomaterials. 2008; 29:3822–3835. [PubMed: 18617258]

Mendonça G, Mendonça DB, Simoes LG, Araujo AL, Leite ER, Duarte WR, Cooper LF, Aragão FJ. Nanostructured alumina-coated implant surface: effect on osteoblast-related gene expression and bone-to-implant contact in vivo. Int J Oral Maxillofac Implants. 2009; 24:205–215. [PubMed: 19492635]

Mendonça G, Mendonça DB, Aragao FJ, Cooper LF. The combination of micron and nanotopography by H2SO4/H2O2 treatment and its effects on osteoblast-specific gene expression of hMSCs. J Biomed Mater Res A. 2010; 94:169–179. [PubMed: 20128007]

Mullin BH, Mamotte C, Prince RL, Wilson SG. Influence of ARHGEF3 and RHOA knockdown on ACTA2 and other genes in osteoblasts and osteoclasts. PLoS ONE. 2014; 9:e98116. [PubMed: 24840563]

Nanci A, Wuest JD, Peru L, Brunet P, Sharma V, Zalzal S, McKee MD. Chemical modification of titanium surfaces for covalent attachment of biological molecules. J Biomed Mater Res. 1998; 40:324–335. [PubMed: 9549628]

Passeri G, Cacchioli A, Ravanetti F, Galli C, Elezi E, Macaluso GM. Adhesion pattern and growth of primary human osteoblastic cells on five commercially available titanium surfaces. Clin Oral Implants Res. 2010; 21:756–765. [PubMed: 20636730]

Prowse PD, Elliott CG, Hutter J, Hamilton DW. Inhibition of Rac and ROCK signalling influence osteoblast adhesion, differentiation and mineralization on titanium topographies. PLoS ONE. 2013; 8:e58898. [PubMed: 23505566]

Salou L, Hoornaert A, Louarn G, Layrolle P. Enhanced osseointegration of titanium implants with nanostructured surfaces: An experimental study in rabbits. Acta Biomater. 2015; 11:494–502. [PubMed: 25449926]

Seo CH, Furukawa K, Montagne K, Jeong H, Ushida T. The effect of substrate microtopography on focal adhesion maturation and actin organization via the RhoA/ROCK pathway. Biomaterials. 2011; 32:9568–9575. [PubMed: 21925729]

Seo CH, Jeong H, Feng Y, Montagne K, Ushida T, Suzuki Y, Furukawa KS. Micropit surfaces designed for accelerating osteogenic differentiation of murine mesenchymal stem cells via enhancing focal adhesion and actin polymerization. Biomaterials. 2014; 35:2245–2252. [PubMed: 24342724]

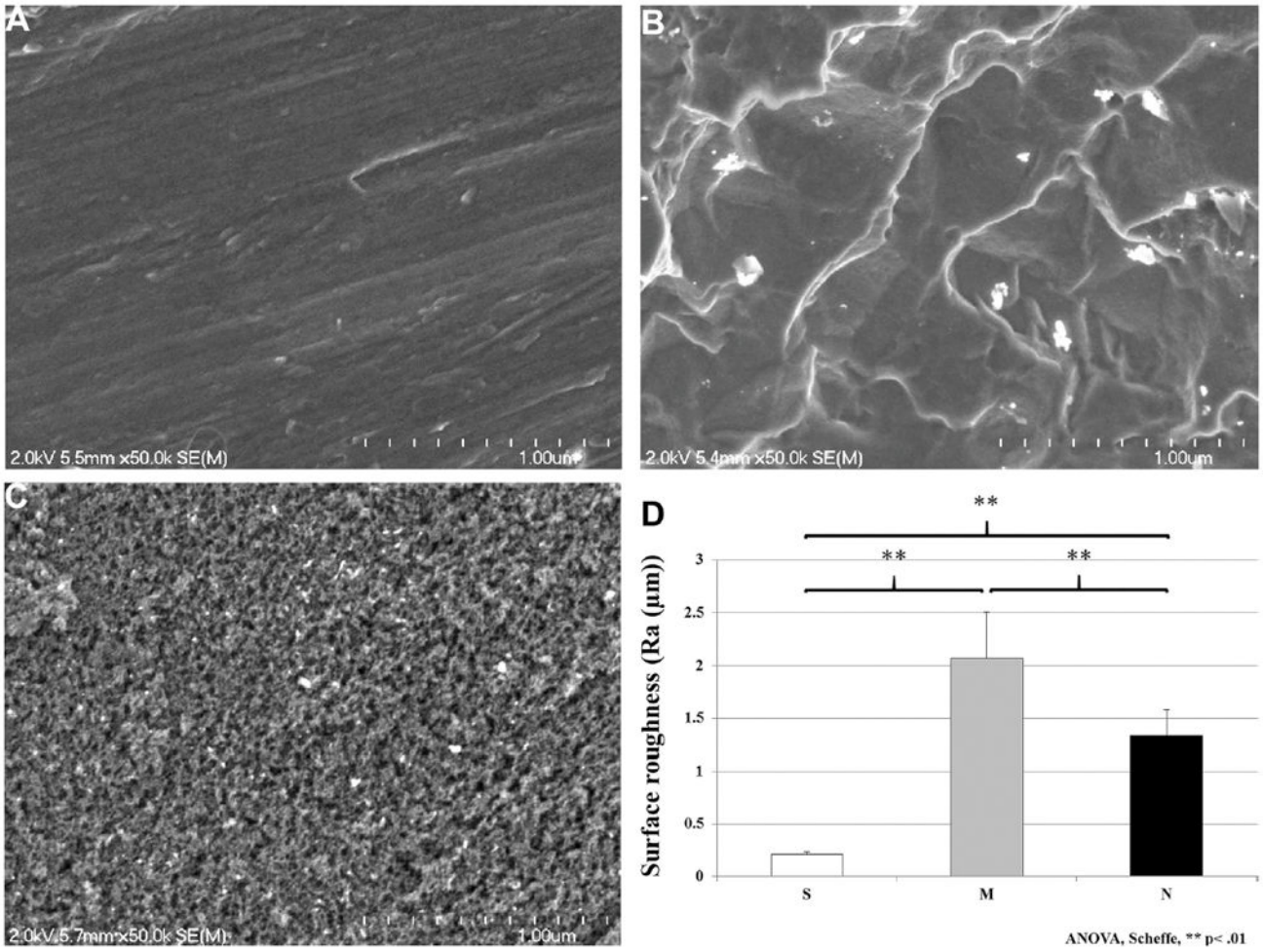

Figure 1.

SEM evaluation of (A) smooth surface (S), (B) microtopography (M), and (C) nanotopography. (D) Surface roughness; Ra: arithmetic roughness (**P < 0.01; ANOVA, Post hoc Scheffe).

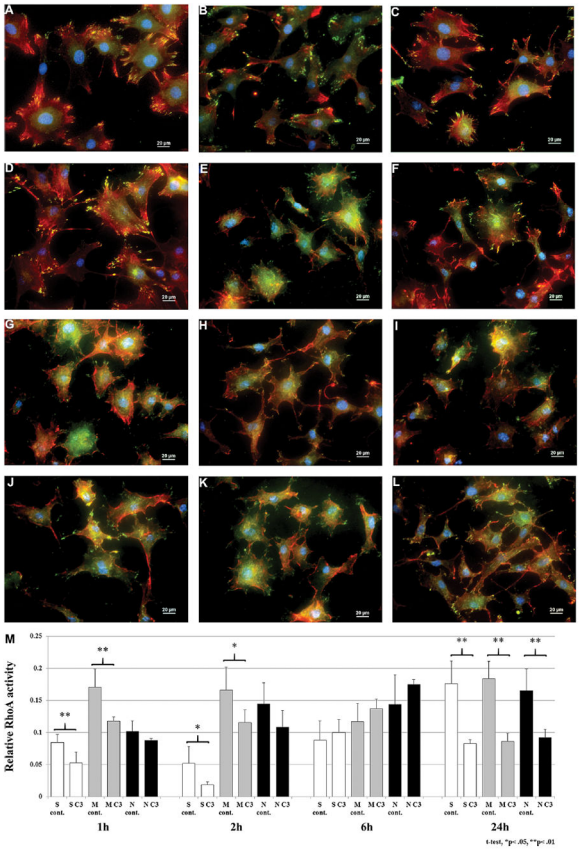

Figure 2.

Fluorescence images showing vinculin (green), actin (red), and nucleus (blue) of the non-treated cells on S (A) at 2 h and (B) at 6 h and C3-treated treated cells on S (C) at 2 h and (D) at 6 h. Non-treated cells on M (E) at 2 h and (F) at 6 h and C3-treated treated cells on M (G) at 2 h and (H) at 6 h. Non-treated cells on N (I) at 2 h and (J) at 6 h and C3-treated treated cells on N (K) at 2 h and (L) at 6 h. (M) RhoA activity during cell adhesion. To evaluate the effect of C3 on RhoA activation on each surface, comparisons between non-treated cells and treated cells on each surface were performed with t test (*P < 0.05; **P < 0.01).

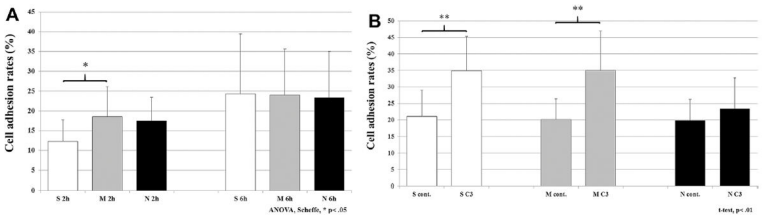

Figure 3.

Cell adhesion assay on each surface. (A) Non-treated cells were seeded on each surface and cultured for 2 and 6 h to quantify the number of the attached cells by MTS assay (*P < 0.05; ANOVA, Scheffe). (B) The number of the attached cell was also demonstrated in the presence of RhoA inhibitor, C3, after 6 h of culture (*P < 0.05; **P < 0.01; T test).

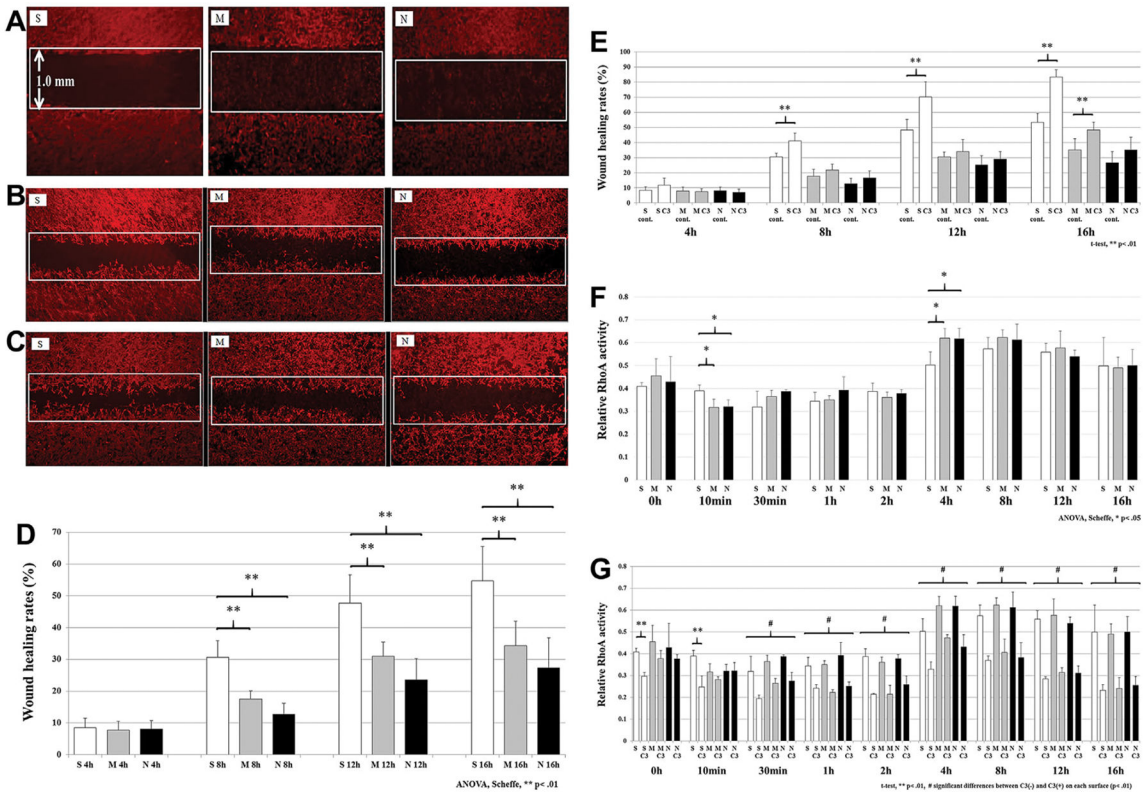

Figure 4.

(A) Fluorescence images after 0 h of scratches. The width of wound area was 1.0 mm and Fluorescence images after 12 h of scratch (B) in the absence of C3 and (C) in the presence of C3. (D) Quantitative analyses of wound healing rate on each surface (n = 6/each group, (**P < 0.01; ANOVA, Scheffe). (E) Quantitative analyses of wound healing rate on each surface in the presence of C3 (**P < 0.01; T test). RhoA activity was determined after scratches for cell migration. Statistical analyses were performed to evaluate (F) the effect of surface topography (**P < 0.01; ANOVA, Scheffe) and (G) the effect of C3 in each surface adherent cells on RhoA activity for 18 h (**P < 0.01, #P < 0.01 on all surfaces; T test).

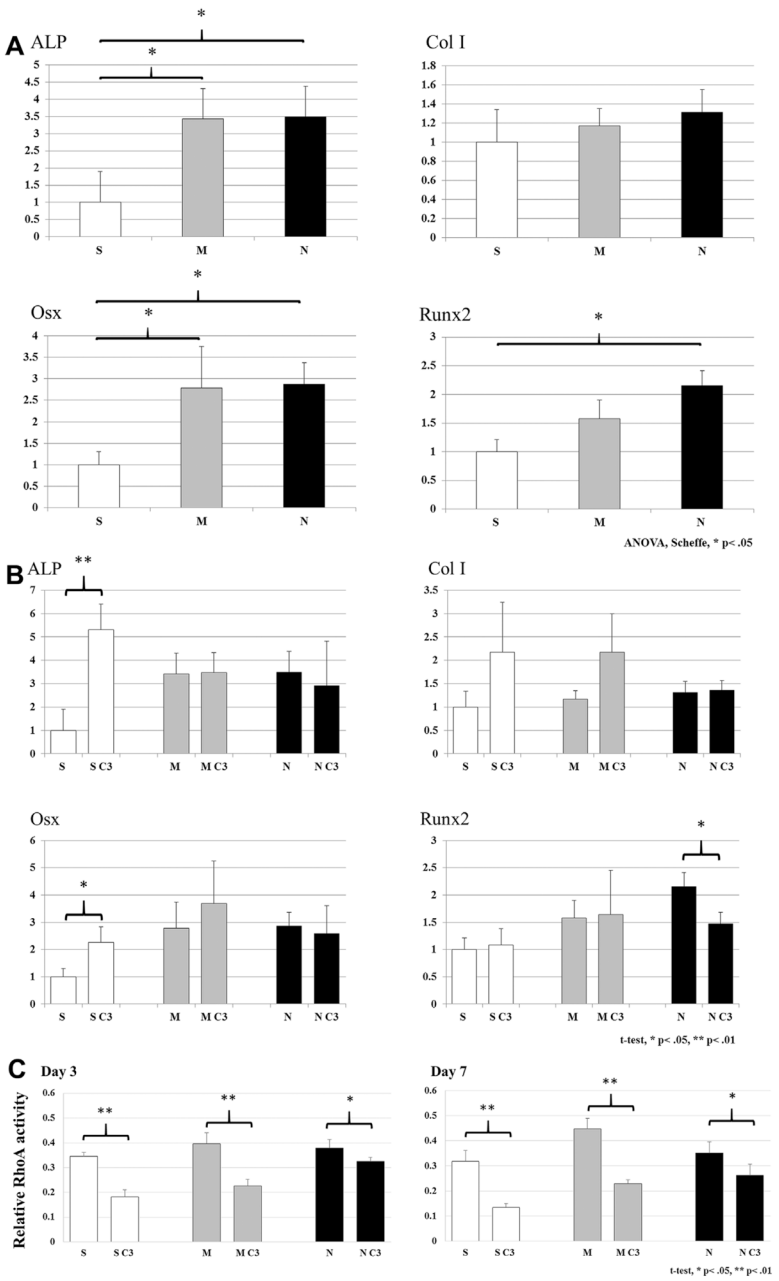

Figure 5.

(A) The effect of surface topography on osteogenic markers expression (*P < 0.05; ANOVA, Scheffe). (B) The effect of C3 on osteogenic markers expression on each surface (*P < 0.05; **P < 0.01; t test). To evaluate the effect of C3 on RhoA activation on each surface, comparisons between non-treated cells and treated cells on each surface (C) in 3 and 7 days were performed with t test (*P < 0.05; **P < 0.01).